

Attenuated-total-reflection Fourier-transformed spectroscopy as a rapid tool to reveal the molecular structure of insect powders as ingredients for animal feeds

Article

Published Version

Creative Commons: Attribution 4.0 (CC-BY)

Open Access

Robertson, K., Ortúñو, J., Stratakos, A., Stergiadis, S. ORCID: <https://orcid.org/0000-0002-7293-182X> and Theodoridou, K. (2024) Attenuated-total-reflection Fourier-transformed spectroscopy as a rapid tool to reveal the molecular structure of insect powders as ingredients for animal feeds. *Journal of Insects as Food and Feed*, 10 (12). pp. 2143-2156. ISSN 2352-4588 doi: 10.1163/23524588-00001092 Available at <https://centaur.reading.ac.uk/116524/>

It is advisable to refer to the publisher's version if you intend to cite from the work. See [Guidance on citing](#).

To link to this article DOI: <http://dx.doi.org/10.1163/23524588-00001092>

Publisher: Wageningen Academic Publishers

the [End User Agreement](#).

www.reading.ac.uk/centaur

CentAUR

Central Archive at the University of Reading

Reading's research outputs online



BRILL
WAGENINGEN
ACADEMIC

JOURNAL OF INSECTS AS FOOD AND FEED (2024) DOI:10.1163/23524588-00001092

Journal of
Insects
as
Food and Feed
brill.com/jiff

RESEARCH ARTICLE

Attenuated-total-reflection Fourier-transformed spectroscopy as a rapid tool to reveal the molecular structure of insect powders as ingredients for animal feeds

K. Robertson¹ , J. Ortuño¹ , A. Stratakos² , S. Stergiadis³  and K. Theodoridou^{1*} 

¹Institute for Global Food Security, Queen's University Belfast, Belfast, BT9 5DL, UK; ²School of Applied Sciences, College of Health, Science and Society, University of the West of England, Bristol, BS16 1QY, UK;

³Department of Animal Sciences, School of Agriculture, Policy and Development, University of Reading, Earley Gate, P.O. Box 237, Reading, RG6 6EU, UK; *k.theodoridou@qub.ac.uk

Received 7 December 2023 | Accepted 20 May 2024 | Published online 12 June 2024

Abstract

Unsustainable agriculture contributes to disastrous global effects – insect-based feed shows potential due to their sustainable, nutritional, and waste upcycling properties. Current EU legislation restricts insect-based meals to fish, pork, and poultry feed; but the near-future shows a great potential for wider acceptance in livestock feed. Black soldier fly larvae (BSFL), mealworm (MW), field cricket (FC), and banded cricket (BC) were sourced within three consecutive weeks – each batch was prepared, freeze-dried, then milled, and stored at -20 °C. Chemical composition of whole-insect meals was analysed for ether extract (EE), crude ash, and nitrogenic contents using standard wet chemistry protocols. Monogastric *in vitro* digestibility was determined through replicating gastric and full intestinal digestion; during this, R-amino acid content was determined through protein hydrolysis kinetics. Additionally, ATR-FTIR was used for molecular analysis, including identification of nutrient-associated functional spectral bands – structural differences were compared through principal component analysis. Insect-based ATR-FTIR analysis demonstrates notable differences in Amide regions, suggesting distinct protein secondary structures, but overall, FC and BC contain the highest crude protein (CP) levels. The lowest CP content was in BSFL; however, BSFL contained the highest ash content – likely consequence of high calcium. Dry matter (DM) yielded lowest in the crickets (FC-28.6; BC-26.9 g/100 g), and highest in MW-38.5 g/100 g; the sum of CP + EE in MW represented >80% DM, but with higher EE contents-CP: EE = 2.45. Data shows greater chitin content in crickets than BSFL + MW. Crickets showed greater neutral detergent fibre (NDF) than BSFL + MW; however, acid-detergent fibre (ADF) was similar among all species, suggesting NDF may include amalgams of interlinked nutrients released by acid digestion. This first study shows for the first time evidence that rearing conditions and substrates influences molecular structure. Exponential solubilisation was observed during pepsin + pancreatin digestion for all, but BSFL exhibited the highest degree-of-hydrolysis during the pancreatin phase, surpassing others. Analysis indicates protein hydrolysis differences are linked to trypsin activity susceptibility.

Keywords

degree of hydrolysis – feed – FTIR – *in vitro* digestibility

1 Introduction

The insect sector can improve the circular economy of the agri-food nexus thanks to their ability to upcycle organic wastes unavailable for human and animal use into valuable biomass, which may be included within food and feed (Chia *et al.*, 2019). Current main interests in using insect-derived products as a feed ingredient lies in its use as a protein-rich sustainable alternative to soybean meal and fishmeal (Sánchez-Muros *et al.*, 2014). EU regulation however, permits the inclusion of insect-derived proteins within fish, pork, and poultry feed exclusively, and only eight species are currently approved: *Hermetia illucens* L. (black soldier fly larvae/BSFL), *Musca domestica* (common housefly), *Tenebrio molitor* (yellow mealworm/MW), *Alphitobius diaperinus* (lesser mealworm), *Acheta domesticus* (house cricket), *Gryllodes sigillatus* (banded cricket/BC), *Gryllus assimilis* (field cricket/FC), and *Bombyx mori* (domestic silkworm) (Regulation (EU), 2021/1372). Additionally, whole live insects, fat, and chitin are insect-derivatives also authorised under EU legislation. Beyond their nutritional value, these raw materials are suggested to impart added value in terms of welfare (live insects), antimicrobial (fat) and prebiotic (chitin) activity (Gasco *et al.*, 2020; Lopez-Santamarina *et al.*, 2020). The expansion of insects as a common raw material in animal feeds will become a reality once legislation enables the inclusion of protein-derived compounds in food-producing animals; however, the insect sector would need to implement the technical advances commonly applied by the feed industry.

Traditional techniques in wet chemistry analysis, adopted to study nutritional value of livestock feeds, are limited by time inefficiency, requirement for extensive sample pre-processing, use of toxic solvents, and the inability to offer complete data. In protein analysis, the destruction of the three-dimensional structures produces information loss at a molecular level, such as protein secondary structures, which influence the utilisation and availability of proteins by gastrointestinal enzymes (Yu, 2005). Attenuated-total-reflectance Fourier-transform infrared-vibration spectroscopy (ATR-FTIR) is a quick, non-destructive, and powerful tool to investigate molecular spectral characteristics of animal feeds without chemically damaging the sample (Theodoridou and Yu, 2013a), and is considered the most accessible technique to study the secondary structure of proteins (Cruz-Angeles *et al.*, 2015). Indeed, protein molecular structures detected by FTIR in common raw materials have been correlated with

protein content, solubility, and intestinal digestibility, which can be used to predict essential nutrient absorption by the small intestine, both in ruminants (Belanche *et al.*, 2013) and monogastrics (Bai *et al.*, 2016). Likewise, FTIR has also been employed to detect molecular differences related to the carbohydrate and lipid profile of vegetable forages related to different cultivars (Krähmer *et al.*, 2021), genetic modifications (Sree *et al.*, 2022), and processing effects (Theodoridou and Yu, 2013b). In entomology, ATR-FTIR, in combination with multivariate analysis, has been traditionally employed for taxonomical purposes (Milali *et al.*, 2019), focusing mainly on profiling cuticular hydrocarbons (Bernardi *et al.*, 2014), and more recently, by direct analysis of insect powders (Mellado-Carretero *et al.*, 2019). Additionally, FTIR combined with multivariate analysis has been successfully applied to predict insects' fatty acid content (Liu *et al.*, 2020). These studies reflect underlying correlations between the spectra features obtained by FTIR, and chemical constituents of interest for the feed industry. However, as of 2023, there is no information regarding the complete molecular profile of powders derived from insects of interest, in respect to their inclusion as a feed ingredient and relationship with the *in vitro* digestibility of monogastric animals. Therefore, the objective this study was to (1) assess the potential of FTIR to reveal the full molecular profile of four insect species permitted for inclusion within animal feeds (BSFL, MW, FC and BC); and (2) investigate the relationship between the molecular structure and chemical profile, and *in vitro* DM and protein degradability.

2 Material and methods

Samples and processing treatments

Three different batches of black soldier fly larvae (BSFL) (*Hermetia illucens*; 10-15 mm, reared on commercial poultry layers mash), Mealworms (MW) (*Tenebrio molitor*; 25-30 mm, reared on wheat grain and carrot), field crickets (FC) (*Gryllus assimilis*; 18-25 mm, reared on sow and weaner pellet) and banded crickets (BC) (*Gryllodes sigillatus*; 14-18 mm, reared on sow and weaner pellet), weighing approximately 200 grams each, were purchased in three consecutive weeks from Livefoods Direct Ltd. (Sheffield, UK). All insects were reared and stored in similar environmental conditions ($23 \pm 0.2^\circ\text{C}$), and food was provided *ad libitum*. Batches were sieved to remove frass and litter, fasted for 12-hours at room temperature ($23 \pm 0.2^\circ\text{C}$), then washed and freeze-dried until constant weight. The dried samples were milled in

a coffee grinder and sieved (<1 mm) (Glennamer sieves Ltd.). Samples were stored at -20 °C pending analysis.

Chemical analyses

Ether extract (EE; 954.02) and crude ash content were measured following the official methods of the Association of Official Analytical Chemists (AOAC). Nitrogen content was analysed using the Dumas method with the Leco Protein/N Analyser (FP-528, Leco Corp., St. Joseph, MI, USA), and crude protein (CP) was calculated using species-specific nitrogenic conversion factors. CP for BSFL was calculated with Nx4.76 by Janssen *et al.* (2017), MW and BC were calculated with Nx5.33 as determined by Boulos *et al.* (2020), and FC was determined with Nx5.0 (Ritvanen *et al.*, 2020). Acid detergent fibre (ADF) and neutral detergent fibre (α NDF) (treated with heat-stable α -amylase (ANKOM Technology Corp., NY, USA), excluding sodium sulphate) were assessed with ANKOM 220 Fibre Analyzer (ANKOM Technology Corp., NY, USA). ADFom and ADIN were analysed by combustion of the ADF residue at 550 °C for 5 hours and Kjeldahl analysis, respectively. ADICP was obtained by multiplying ADIN by 6.25. The chitin content (%DM) was estimated by ash-free ADF (%) - ADICP (%) (Marono *et al.*, 2015). Lignin (sulphuric acid) (ADL) was analysed according to Van Soest *et al.* (1991).

In vitro apparent digestibility

A three-step method was applied to simulate gastric and full intestinal digestion based on a modified version by Boisen and Fernández (1997). Samples were weighed at 0.5 ± 0.1 g in triplicate in ANKOM F57 bags (ANKOM Technology Corp., NY, USA), and introduced into 250 mL glass flasks with a screw cap. Phosphate buffer (25 mL, 0.1 N; pH 6.8) and 10 mL of 0.2 N HCl solution were added to the flask and the pH adjusted to 2. Further, 1 mL (25 mg/mL) of freshly-prepared pepsin (P-7000, Sigma-Aldrich, St. Louis, MO, USA) and 0.5 mL of chloramphenicol (0.5 g/100 mL ethanol) were added to the flasks, and incubated at 39 °C for 2 h with magnetic agitation. Post-incubation, 10 mL of 0.2 N phosphate buffer (pH 6.8) and 5 mL of 0.6 N NaOH were added; the pH was adjusted to 6.8. 2.5 mL of fresh pancreatin (P-1750, Sigma-Aldrich) solution (40 mg/mL) was added, and incubation proceeded at 39 °C for 4 h. After the second incubation, 10 mL of a 0.2 M EDTA solution was added to the flask, and the pH adjusted to 4.8 with 30% acetic acid solution. 0.5 mL of Viscozyme (multienzyme complex from *Aspergillus aculeatus* containing cellulase) was added, and the flask incubated again at 39 °C for 18 h. Finally, filter bags with the sample were

removed and submerged, sequentially, with distilled water (2×50 mL/sample), 95% ethanol (20 mL/sample), and acetone (20 mL/sample) for 2 minutes. Then, filter bags were dried (80 °C \times 24 h) and weighted to calculate total tract dry matter digestibility. Digestions were run in triplicate for each batch and digestion phase (soluble, pepsin, pancreatin, Viscozyme), for a total of 9 replicates for sample species.

Degree of protein hydrolysis kinetics

Samples (1 mL) were taken at different intervals prior to pepsin (soluble fraction) and pancreatin addition; and during pepsin (12, 30, 45, 60, 90 and 120 min) and pancreatin *in vitro* digestion (30, 60, 90, 120, 180 and 240 min) as previously described. Slightly modified method of Benjakul and Morrissey (1997) was used to determine R-amino acid content. Properly diluted samples (125 μ L) were mixed thoroughly with 2 mL of 0.2125 M phosphate buffer, pH 8.2, followed by the addition of 1 mL of 0.01% TNBS solution. The mixtures were then placed in a thermoblock at 50 °C for 30-minutes in darkness. The reaction was terminated by adding 2 mL of 0.1 M sodium sulphite. The mixtures were cooled at ambient temperature for 30 minutes. The absorbance was measured at 420 nm, and R-amino acid was expressed in terms of L-leucine. The DH was defined as follows: $DH_t = [(L_t - L_0)/(L_{max} - L_0)] \times 100$ (1); where L_t corresponded to the amount of R-amino acid released at time t . L_0 was the amount of R-amino acid at the beginning of digestion; L_{max} was the maximum amount of R-amino acid obtained after enzyme hydrolysis. Total hydrolysis was performed by adding 5 mL 6 N HCl to 50 ± 2 mg of undigested dried insect powder and incubated at 100 °C for 24 h under reflux. The acid-hydrolysed sample was filtered through Whatman paper no. 1 to remove unhydrolysed debris. The supernatant was neutralised with 6 N NaOH before R-amino acid determination.

The kinetics of R-amino acid were described using a linear equation: $D_t = D_0 + mt$ (3); where D_t is the fraction of a dietary component digested at time t (min.), D_0 is the fraction of protein soluble at the initial stages, and m is the fractional digestion rate (per min.). The kinetics of R-amino acid solubilisation during the pepsin + pancreatin stage digestion were described by an exponential model: $DC_t = D_i \times (1 - \exp(-k \times t)) + D_{i-1}$ (2); where DC_t is the fraction of a dietary component digested at time t (min.), D_i the fraction of a protein that can be potentially digested during enzymatic digestion, D_{i-1} the fraction of protein that was digested prior to the enzymatic digestion; and k is the fractional digestion rate

(per min.). Model parameters were estimated using the non-linear modelling of PAST 4.01 software (Paleontological Statistics Software Package, University of Oslo, Norway) and the parameters estimates were then statistically compared.

FTIR data and collection analysis

FTIR collection was performed at ambient temperature using a Nicolet iS5 FTIR spectrometer and ATR iD7 accessory (Thermo Fisher Scientific, Dublin, Ireland), with diamond crystal, ZnSe lens, and DTGS KBr detector. After the sample holder was cleaned with an alcohol swab, the samples were placed on the crystal facet while the slip clutch tower applied equal pressure. Sixty-four scans per sample were collected in the mid-infrared range from 550 to 4,000 cm^{-1} in transmission mode at a spectral resolution of 4 cm^{-1} . The collected spectra were corrected against air as background. Five replicates of each sample were measured and averaged before data pre-processing. Before the measurements of peak heights and areas, each IR spectrum was normalised, and then its second derivative was generated and auto-smoothed (Supplementary Figure S1). The collection of the functional spectral bands associated with nutrient molecular structures, the corrections with the background spectrum and the data pre-processing were completed with OMNIC 7.3 software (Spectra-Tech Inc., Madison, WI, USA). The five spectra of each insect sample along with its second derivatives were saved in .csv files.

Univariate molecular analysis

The functional spectral bands associated with lipid and protein molecular structures were identified with OMNIC 7.2 software (Spectra-Tech Inc., Madison, WI, USA) and assigned according to published studies (Figure 1):

1. Carbohydrate (CHO, ca. 1,485-950 cm^{-1}): further divided into total carbohydrate (TC, ca. 1,185-950 cm^{-1}) region, containing three major peaks at ca. 1,157 (TC3), 1,114 (TC2) and 1,078 (TC1) cm^{-1} ; and structural carbohydrate (STC, ca. 1,485-1,285 cm^{-1}), with three major peaks at ca. 1,466 (STC3), 1,455 (STC2) and 1,393 (STC1). Each sub-carbohydrate region was measured according to its baselines.
2. Protein structure comprised the primary and secondary structures. The primary protein structures included Amide I (AmI; ca. 1,637 cm^{-1}), Amide II (AmII; ca. 1,540 cm^{-1}) and Amide III (AmIII; ca. 1,238 cm^{-1}). The baseline of Amide I and II spectral

was centred at ca. 1,710-1,485 cm^{-1} , and at 1,285-1,185 cm^{-1} for Amide III, and were used to calculate the spectral heights. The heights for the secondary protein structures were determined by using the second derivative function in OMNIC, according to published methods. 12,19 α -helix (αH) and β -sheet (βS) peaks fell at ca. 1,655 and 1,633 cm^{-1} , respectively. The $\alpha\text{H}/\beta\text{S}$ and AmI/AmII ratios were calculated.

3. Lipid-related region comprises two parts: carbonyl C = O region (CCO, ca. 1,770-1,710 cm^{-1}) and (a)symmetric CH_2 and CH_3 region (ASCC, ca. 3,050-2,760 cm^{-1}). The CCO centre at ca. 1,735 cm^{-1} , while ASCC features contains four major peaks at ca. 2,959 cm^{-1} (asymmetric CH_3 , AsCH₃), 2,916 cm^{-1} (asymmetric CH_2 , AsCH₂), 2,873 cm^{-1} (symmetric CH_3 , SyCH₃), and 2,848 cm^{-1} (symmetric CH_2 , SyCH₂). Areas of carbonyl C = O region (CCOA) and (a)symmetric CH_2/CH_3 region (ASCCA) were also measured according to their baselines and CH_2/CH_3 ratio was calculated.

Multivariate analysis

Principal component analysis (PCA) was performed including the CHO, amide and lipid regions of IR spectra to compare and distinguish inherent structural differences between insects. PCA results were plotted based on the two highest factor scores (PC1/PC2) and presented as a function of those scores. 95% confidence ellipses were calculated and displayed for each group (leaves/stems; cultivars) in the PCA plots. PCA analysis was carried out using PAST 4.01 software. PC1 and PC2 loadings correlations are included in Supplementary Figure S1.

Statistical analysis

One-way analysis of variance (ANOVA) was performed for the chemical composition, univariate molecular structure and digestibility analysis using the statistical package of SPSS 25 (IBM Software Group, Chicago, IL, USA). All assumptions of ANOVA were met. Significance was declared at $P < 0.05$, and trends were declared at $P \leq 0.10$. When significant, means with different letters among cultivars were obtained using Duncan's test. The correlation between the molecular structure profiles and the wet chemical analysis in the insect samples were analysed using Pearson's correlations. Normality test of residual data was conducted using the Shapiro-Wilk's method.

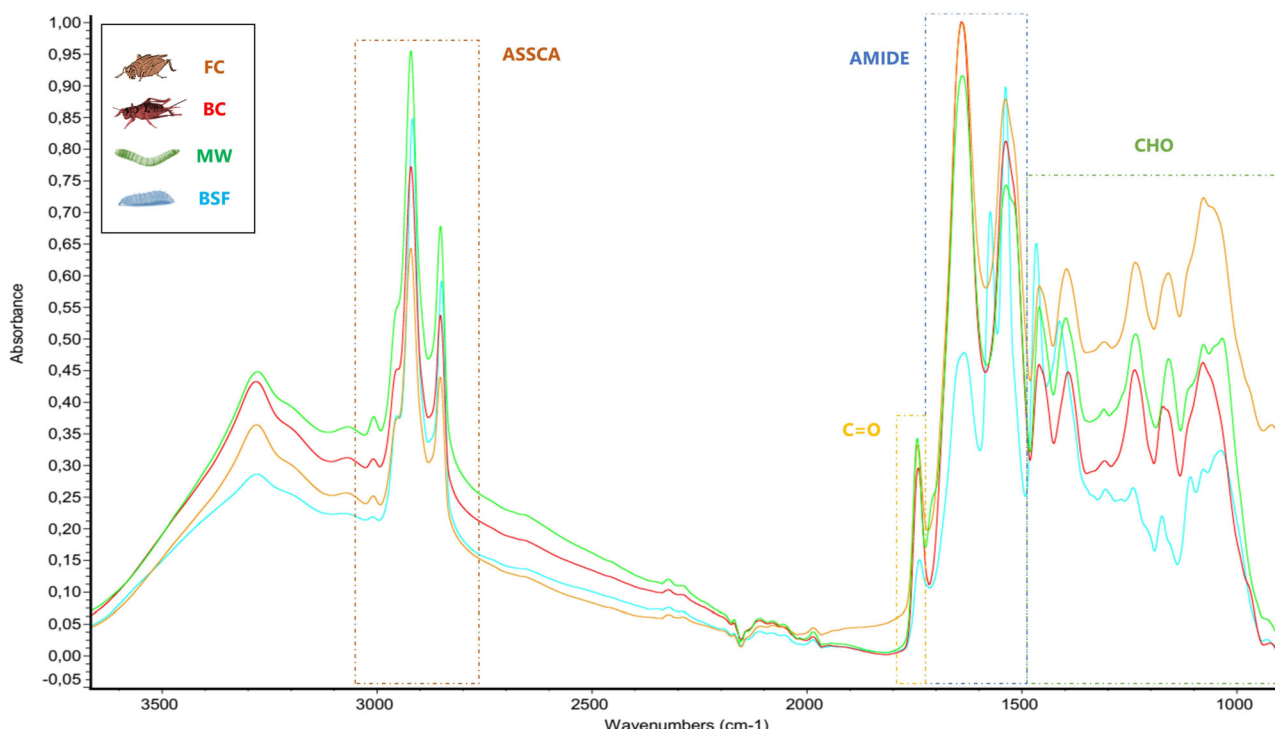


FIGURE 1 Average MIR spectra ($950\text{--}4,000\text{ cm}^{-1}$) of the whole-insect meals from BSFL, MW, FC and BC.

3 Results and discussion

Chemical composition

Table 1 shows the averaged chemical composition of the different batches of insect species. The chemical constituents' values are within the range of BSFL larvae (Meneguz *et al.*, 2018) and MW range (Marono *et al.*, 2015). FC contents were similar for CP and EE but higher for ash and chitin/fibre than previous studies (Zielińska *et al.*, 2015; Ribeiro *et al.*, 2019). Fewer studies focus on BC's composition; however, comparable nutritional contents to the present study were observed in data found for this species (Jayanegara *et al.*, 2017). Dry matter nutritional parameters were similar when compared between cricket species, which was mainly characterised by a CP content above 50% and EE between 20-25% (ratio CP:EE = 2.45 and 2.09 for FC and BC, respectively). The sum of CP plus EE in MW also represented more than 75% DM, but with a higher EE content (CP:EE = 1.22). In contrast, BSFL showed the lowest CP content with a similar EE to MW (CP:EE = 0.95). The content of ash was highest ($P < 0.05$) in the BSFL, which is coherent with values obtained in literature, and likely related to the high calcium content, giving them the suitable common name of 'Calcigrubs'. Among the other species, MW showed the lowest ash content ($P < 0.05$), and both cricket species showing intermediate levels ($P < 0.05$), but no significant

species-specific difference. Regarding structural carbohydrates, both *Gryllidae* showed more than double NDF than BSFL and MW. However, the content of ADF was similar among all the species, suggesting that NDF may include an amalgam of interlinked carbohydrates, proteins, and minerals, that can be further released by acid digestion. NDF and ADF's significance is still not completely identified in insects as it is in vegetable feeds. For ADF, it is generally considered that after the subtraction of the mineral (ADFom) and protein content (ADICP) it reflects the content of chitin, a similar structure to that of cellulose (Marono *et al.*, 2015). According to this estimation, both crickets showed higher ($P < 0.05$) chitin content than BSFL and MW. The residue obtained after digestion with concentrated sulfuric acid (ADL), related to ligniferous substances in forages, was similar in all species.

Molecular nutritional profile

Figure 1 shows the normalised mid-infrared (MIR) spectra ($3,600\text{--}900\text{ cm}^{-1}$) obtained by ATR-FTIR of the four studied insect species. Amplified images of the different regions of interest with greater detail on the absorbance bands can be found in Supplementary Figure S2. In previous studies, the application of ATR-FTIR to the complete body of different insect species yielded comparable MIR spectra profiles (Mellado-Carretero *et al.*, 2019). Overall, two regions presented the highest inten-

TABLE 1 Chemical composition of the whole-insect meals from BSF, MW, FC and BC

g/100 g DM	Insect species				SEM	P
	BSF	MW	FC	BC		
DM (g/100 g)	35.2 ^a	38.5 ^a	28.6 ^b	26.9 ^b	1.59	**
EE	31.3 ^{ab}	35.0 ^a	21.8 ^c	25.3 ^{bc}	1.82	*
CP	29.7 ^c	42.7 ^b	53.5 ^a	52.9 ^a	2.99	***
ASH	13.0 ^a	4.69 ^c	8.58 ^b	7.06 ^b	1.050	**
NDF	13.2 ^b	11.7 ^b	35.2 ^a	32.3 ^a	3.31	***
ADF	9.33 ^{bc}	8.36 ^c	15.6 ^a	12.1 ^{ab}	0.954	**
ADICP	4.06 ^b	4.38 ^b	9.81 ^a	5.75 ^{ab}	0.338	**
ADL (H ₂ SO ₄)	1.17	1.44	1.50	1.16	0.104	NS
Chitin	5.83 ^b	4.86 ^b	7.70 ^a	7.41 ^a	0.506	*

sity of absorbance bands: 1,710-1,485 cm⁻¹ and 3,050-2,750 cm⁻¹. The former is associated with the Amide region, which includes unique primary protein features of peptide bonds: Amide I (\approx 80% C = O and \approx 20% C-N stretching vibration, centred at a wavelength of ca. 1,640 cm⁻¹) and Amide II (\approx 60% N-H bending vibration and \approx 40% C-N stretching vibration; ca. 1,535 cm⁻¹) (Theodoridou *et al.*, 2013b). An extra Amide III region can be found between 1,285-1,185 cm⁻¹ with the peak centred at ca. 1,238 cm⁻¹, related to C-N stretching and N-H bending vibrations (Stani *et al.*, 2020). These three regions have been related to protein features in different insect species sections by FTIR (Khoshmanesh *et al.*, 2017; Mellado-Carretero *et al.*, 2017). FC showed the highest AmIH, followed by BC and MW, showing BSFL the lowest value (Table 2). In contrast, the Amide II height was greater in BSFL, followed by the two crickets, and MW ($P < 0.05$). For the Amide III, the pattern responded to MW = FC > BC > BSFL. Finally, the whole Amide area (ca. 1,710-1,485) showed the highest values for both crickets, followed by MW, and showing BSFL the lowest content. Although the amide spectra profile of MW, FC and BC showed a similar pattern, the AmII region in BSFL presented an extra peak centred around 1,575 cm⁻¹. Little data is available regarding the application of FTIR to whole BSFL larvae. Up to the knowledge of the authors, this peak has not been previously detected in FTIR spectra of other insect species samples (Khoshmanesh *et al.*, 2017; Mellado-Carretero *et al.*, 2017), or whole heat-treated BSFL larvae analysed by the same team (Campbell *et al.*, 2020). Insect chemical profile, and potentially molecular profile, is influenced by rearing conditions (Chieco *et al.*, 2019), as detected by FTIR techniques; therefore, the rearing environment and feed might explain the presence of this artefact peak.

AmI band is particularly sensitive to protein secondary structure, and thus, is generally used to predict protein secondary structure (Yu, 2005). The absorption heights of α H (ca. 1,655 cm⁻¹) and β S (ca. 1,623 cm⁻¹) can be rapidly detected using the second-derivative function (Theodoridou *et al.*, 2013b) (Supplementary Figure S2). Both α H and β S proportions followed a similar pattern: FC > BC = MW > BSFL. The relationship of proportions between both major protein secondary structures might be related to the protein's nutritive value (Doiron *et al.*, 2009). Different proteinaceous feed materials have shown to contain different proportions of α H/ β S ratios, which were correlated with different protein solubility and digestibility. Likewise, feed processes might affect the proportion of both structures. For instance, the application of heat may increase the content of β S in detriment of α H, which can reduce the protein digestibility. In the present study, the α H/ β S ratio showed no differences between freeze-dried insect species; however, a different ratio discovered in previously heat-dried BSFL and MW reveals a significant correlation between protein digestibility (Campbell *et al.*, 2020).

The 3,050-2,760 cm⁻¹ (ASCC) and 1,780-1,710 cm⁻¹ (CCO) bands are generally related to symmetric and asymmetric stretches of alkyl chains (CH₂ and CH₃) and ester carbonyl (C = O) vibrations, respectively, and thus, to the presence of lipids. Indeed, both ASCC and CCO represented the major absorbance bands when FTIR was applied to insect oil samples (Tiencheu *et al.*, 2012; Liu *et al.*, 2020) – symmetric and asymmetric stretch vibration peaks within the ASCC region showed higher intensities ($P < 0.05$) for BSFL and MW than for cricket species. However, the peak centred ca. 3,008, associated with the lipid unsaturation degree, showed a different pattern: MW > FC = BC > BSFL. The height of the peak related to ester carbonyl vibrations (ca. 1,742) was lowest for BSFL in comparison with the other species, which showed no differences ($P > 0.05$) among them. Finally, two other bands were observed in the 'fingerprint' region: STC (1,485-1,285 cm⁻¹) and TC (1,185-950 cm⁻¹). Both bands are commonly associated with carbohydrates in different insect sections (Balan *et al.*, 2019; Mantilla *et al.*, 2020; Bernardi *et al.*, 2014). The STC is linked to asymmetric bends and stretching deformation vibrations of CH₂ and CH₃ groups, mostly linked to the insects' cuticle, and structural carbohydrates in forages. The TC region is associated to bending vibrations of in-plane C-H groups and can be related to the presence of polysaccharides and sugars; and thus, might be more influenced by the substrate and rearing condi-

TABLE 2 Molecular profile of the whole-insect meals from BSF, MW, FC and BC

cm ⁻¹	Insect species				SEM	P
	BSF	MW	FC	BC		
Carbohydrate region (ca. 1,485-940)						
TC_A	26.44	27.81	25.04	24.49	0.7141	NS
TC1	0.218	b	0.369	a	0.352	a
TC2	0.190	b	0.273	a	0.221	ab
TC3	0.302	a	0.301	a	0.255	ab
STC_A	14.33	b	16.62	a	13.90	b
STC1	0.216		0.253		0.192	
STC2	0.255	a	0.232	b	0.162	c
STC3	0.425	a	0.227	b	0.141	c
Lipid-related regions						
CO_A	1.744	b	4.618	a	4.230	a
C = O	0.101	b	0.245	a	0.199	ab
ASSC_A	39.81	a	43.60	a	33.19	b
ULB	0.009	c	0.039	a	0.022	b
AsyCH3	0.194	ab	0.223	a	0.185	b
AsyCH2	0.705	a	0.694	a	0.513	b
SyCH3	0.173	ab	0.187	a	0.146	bc
SyCH2	0.489	a	0.447	a	0.325	b
CH ₂ /CH ₃ H	3.267	a	2.787	b	2.526	c
Amide region (ca. 1,485-1,700)						
AmideA	52.94	c	70.89	b	86.73	a
AmI	0.311	c	0.644	b	0.810	a
AmII	0.773	a	0.440	c	0.550	b
AmIII	0.121	c	0.301	a	0.276	a
AmI/AmII	0.407	b	1.468	a	1.474	a
α-Helix	0.307	c	0.609	b	0.778	a
β-Sheet	0.303	c	0.599	b	0.756	a
αH/βS	0.998		1.018		1.029	
					1.040	0.0124
						NS

tions (Mantilla *et al.*, 2020). BSFL showed the highest intensities in the STC2 and STC3, whereas MW heights were highest for STC1. Major peaks in the TCA band showed more variability between species, although, in general, MW showed the highest intensities. All the peaks detected in the present study have been previously observed in the FTIR spectra from different insect species (Johnson, 2020).

In vitro dry matter digestibility (DMd)

Figure 2 shows the average DMd of the whole-insect meals from BSFL, MW, FC and BC divided by the different stages of simulating *in vivo* monogastric digestion: soluble, gastric (pepsin; pH = 2), small intestine (pancreatin; pH = 6.8) and large intestine (Viscozyme; pH = 4.8). MW showed the highest DMd (81.2%; $P < 0.05$) in comparison with the other species, which showed

values around 70%. However, the pattern of the different steps greatly varied between them. MW showed the highest soluble fraction (almost 30%), not statistically different from BSFL, and with crickets showing values below 15%. Whereas no differences ($P > 0.05$) were found during the gastric stage – the pancreatin DMd in both cricket species represented up to 30% of total DMd, much higher ($P < 0.05$) than for MW (<20%) and BSFL (<10%). In contrast, the fraction digested by the Viscozyme complex was highest in the BSFL larvae (23.8%) ($P < 0.05$), and similar (8-10%) between the others. Similar values for DMd of BSFL (60-85%) (Bosch *et al.*, 2016; Campbell *et al.*, 2020; Zhen *et al.*, 2020), MW (76-92%) (Bosch *et al.*, 2016; Poelaert *et al.*, 2016) and house cricket (*Acheta domesticus*) (56-60%) (Poelaert *et al.*, 2016) obtained in previous studies by similar *in vitro* techniques have been previously found. Besides,

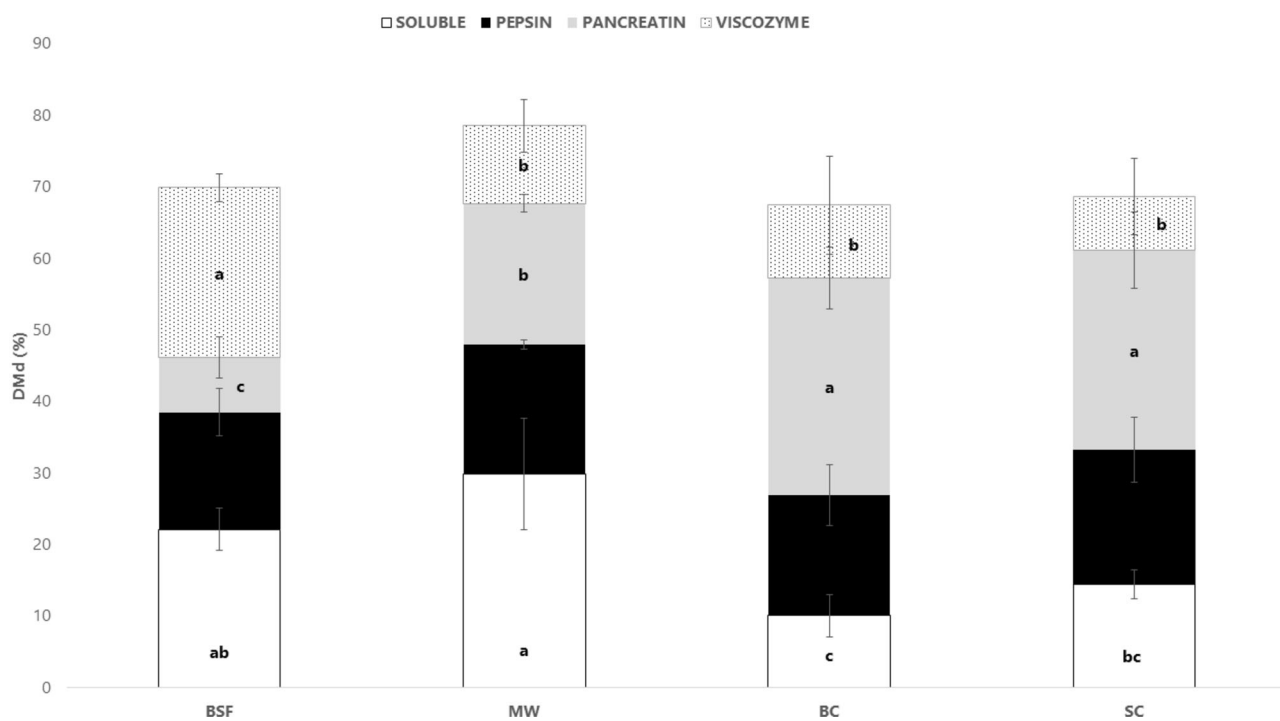


FIGURE 2 *In vitro* dry matter digestibility of the whole-insect meals from BSFL, MW, FC, and BC.

TABLE 3 Estimates of the protein degree of hydrolysis kinetics of the four insect species under analysis during the pepsin and pancreatin phase of the digestion

DH solubilisation	Insect species				SEM	P
	BSFL	MW	FC	BC		
Pepsin						
Soluble _{DH} (%)	10.9	11.5	8.28	11.4	1.065	NS
ΔD _{DH}	14.5	13.8	14.9	14.9	0.903	NS
D _{max}	25.4	25.2	23.2	26.3	0.657	NS
m (min ⁻¹)	0.12	0.11	0.12	0.12	0.008	NS
Pepsin + pancreatin						
D ₀ (%)	25.2	23.2	20.7	22.8	0.824	NS
ΔD _{DH}	10.4	^a 6.54	^{ab} 4.64	^b 4.00	^b 1.004	*
D _{max}	35.6	^a 29.7	^b 25.4	^b 26.8	^b 1.541	**
k (min ⁻¹)	0.15	0.19	0.30	0.17	0.003	NS

when these insect species were compared, MW showed higher DMd than BSFL and crickets (Kovitvadhi *et al.*, 2019; Bosch *et al.*, 2016; Poelaert *et al.*, 2016). No previous information was found either for FC or BC. To author knowledge, this is the first study exploring the kinetics of the different DMd phases in insects, and thus, no comparison can be made with previous references. However, the evaluation of organic matter digestibility in common raw feed materials showed a similar digestibility pattern of cricket species to that of wheat bran (Wilfart *et al.*, 2007).

Degree of hydrolysis

Table 3 shows the degree of hydrolysis of the four insect species' solubilised proteins during the sequential incubation with pepsin and pancreatin. The R-amino solubility during the pepsin digestion followed linear kinetics whereas pepsin + pancreatin showed exponential solubilisation trends. Boukil *et al.* (2020) previously found similar N solubilisation kinetics during pepsin hydrolysis for MW, although they found an exponential trend for BSFL proteins. In both cases, exponential solubilisation was found during pepsin + pancreatin digestion. In the present study, no differences ($P > 0.05$)

were found between the insect species at the soluble or pepsin (ΔD_{DH}) digestibility, showing similar solubilisation rates (m) and reaching maximum values (D_{max}) between 23.2-26.3%. However, BSFL showed the highest DH during the pancreatin phase (10.4%), significantly different than both crickets species and with MW with intermediate values ($P > 0.05$). As a result, the final R-amino acid solubilisation at the end of the enzymatic DH was higher for BSFL ($P < 0.05$) in comparison to other species. The DH has been successfully employed for the quantification of the protein *in vitro* digestibility following similar methods in different insect's species (Manditsera *et al.*, 2019; Purschke *et al.*, 2018; Leni *et al.*, 2019). The values obtained in the present study were in line with those obtained for BSFL, MW, and crickets (*Henicus whellani*), with values between 15-30% (Manditsera *et al.*, 2019; Janssen *et al.*, 2019). Indeed, when directly compared, BSFL soluble proteins already showed a higher DH than MW (Janssen *et al.*, 2019). In addition to our study, differences in protein hydrolysis seem to be related to the susceptibility to trypsin activity (a pancreatic protease), whereas no differences were observed after pepsin digestibility.

Correlations between spectra parameters and nutrition profiles of the insect species

Table 4 shows the correlations between spectral parameters found and the chemical components of the four insect species. The most relevant finding is related to the strong positive correlation ($r > 0.95$; $P < 0.001$) found between the height of the AmI, β S, α H/ β S and the AmideA with the CP content. These spectra parameters were also correlated ($r > 0.65$; $P < 0.01$) with the ADICP, NDF and ADF. However, no correlation ($P > 0.05$) was found with the chitin content, free of ADICP. These results suggest a high content of CP in the NDF/ADF fractions. The possibility of predicting CP content employing the Amide region are in line with the results observed in previous studies applying FTIR to feedstuff samples (Liu *et al.*, 2013; Vandanon *et al.*, 2023). This finding represents a suitable outcome for applying FTIR to quality control in the analysis of insect powders intended as animal feed due to the relevance of the total and accessible CP content. On the other hand, the chitin content showed only a modest correlation ($r = 0.58$; $P < 0.05$) with the α H/ β S ratio. According to literature, α -chitin is characterised by three prominent peaks located around $1,650\text{ cm}^{-1}$, $1,620\text{ cm}^{-1}$, and $1,554\text{ cm}^{-1}$; the two formers coinciding with peaks commonly related to protein secondary structures. The higher CP content in whole insect samples might hin-

der the analysis of chitin by FTIR techniques. Further research would be needed to clarify this issue.

Within the ASCCA region, we observed a negative correlation ($r < -0.60$; $P < 0.01$) between AsyCH₂, SyCH₂ and CH₂/CH₃, and the CP, NDF and ADF contents; whereas a modest positive correlation ($r > 0.55$; $P < 0.01$) was found with the EE content, which has been previously related (Liu *et al.*, 2020). A similar pattern was found in some typical CHO area peaks, such as at $1,157$ and $1,455\text{ cm}^{-1}$. These frequencies are related to asymmetric CH₂ and CH₃ stretching deformations and in-plane C-H bends, shared in lipids and carbohydrates (Bernardi *et al.*, 2014; Antoniali-Junior *et al.*, 2007). Overall, the results showed different significant correlations between chemical constituents and spectral features, revealing the possibility of using FTIR for the proximal composition profiling of insect powders.

The correlations found between DM digestibility coefficients and spectra parameters revealed the differences in digestibility during each phase. The peaks $1,393$, $1,455$, AsyCH₃, SyCH₂ and ASCCA region were positively correlated ($r > 0.55$; $P < 0.05$) with the soluble fraction of the insects, indicating the positive correlation found with the EE (see Supplementary Figure S1). Likewise, the digestibility during the pancreatin phase seemed to be negatively correlated ($P < 0.01$) with the content of CP ($r = -0.99$), but positive for NDF ($r = 0.80$), which was reflected in the significant correlations found between these chemical constituents and spectral features, especially AmI, α H/ β S ($r > 0.90$) and $1,466\text{ cm}^{-1}$ and CH₂/CH₃ ($r < -0.90$).

Finally, no differences were found between the pepsin DH parameters or the total DH. However, the spectral parameters correlated with pancreatin DMd showed a similar, but opposite correlation with the amino acid solubilisation occurred during pepsin + pancreatin DH (PanDH) and at the end of the enzymatic digestion (TotDH). AmI, α H, β S, $1,466\text{ cm}^{-1}$, and CH₂/CH₃ showed a strong correlation with CP, NDF, ADF and ADICP content. But, PanDH was only negatively correlated with CP ($r = -0.75$) and NDF ($r = -0.69$), whereas TotDH, was also correlated with ADF ($r = -0.66$) and chitin ($r = -0.65$). These findings suggest that most soluble protein content is digested by pepsin, whereas the CP content included in NDF (NDICP, not quantified in the present study) might be less accessible for enzymes during further digestion.

Principal component analysis

Figure 3 shows the representation of the two first PCs (94% of variance explained) obtained by multivari-

TABLE 4 Correlation scores between chemical composition and FTIR spectra values

	TC_A	TC1	TC2	TC3	STC_A	STC1	STC2	STC3	AmideA	AM1	AM II	AM III	AmI/ AmII	ah	bs	aH/bS	C = O	CO_A	ASC_A	ULB	AsyCH ₃	SyCH ₂	SyCH ₃	CH ₂ CH ₃ H	
CP	-0.62	0.87	-0.89	-0.82	0.16	-0.48	-0.95	-0.98	0.99	0.97	-0.73	0.69	0.89	-0.36	0.96	0.96	0.75	-0.63	0.88	-0.93	-0.47	-0.87	-0.72	-0.93	-0.99
ADICP	-0.18	-0.22	0.20	-0.55	0.27	-0.31	-0.67	-0.59	0.75	0.69	-0.21	0.40	0.47	0.71	0.71	0.30	0.26	0.45	-0.49	-0.07	-0.27	-0.55	-0.45	-0.57	-0.61
EE	0.29	0.42	0.00	0.75	-0.02	0.29	0.74	0.53	-0.65	-0.57	0.10	-0.16	-0.32	-0.61	-0.58	-0.61	-0.03	-0.22	0.59	0.30	0.40	0.59	-0.53	0.59	0.57
ASH	-0.04	-0.68	-0.79	0.01	-0.48	-0.31	0.25	0.61	-0.05	-0.59	0.87	-0.78	-0.77	-0.58	-0.57	-0.32	-0.77	-0.70	-0.17	-0.87	-0.37	0.09	-0.19	0.20	0.58
NDF	-0.51	-0.38	0.16	-0.64	-0.09	-0.57	-0.89	-0.72	0.79	0.72	-0.28	0.29	0.52	0.73	0.72	0.40	0.28	0.49	-0.75	-0.13	0.51	-0.80	-0.68	-0.81	-0.77
ADF	-0.09	-0.26	0.20	-0.63	0.09	-0.45	-0.72	-0.57	0.70	0.65	-0.16	0.30	0.41	0.68	0.66	0.51	0.28	0.47	-0.56	-0.20	-0.33	-0.60	-0.50	-0.61	-0.63
CHITIN	0.04	-0.17	0.17	-0.51	0.15	-0.49	-0.57	-0.41	0.46	0.42	-0.10	0.12	0.26	0.46	0.42	0.58	0.27	0.40	-0.48	-0.23	-0.31	-0.50	-0.41	-0.50	-0.59
ADL	0.24	0.26	0.31	-0.13	0.59	0.35	-0.10	-0.22	0.33	0.33	-0.25	0.42	0.30	0.34	0.35	0.17	0.27	0.27	0.18	0.25	0.33	0.07	0.21	0.02	-0.26
SolDMd	0.38	-0.25	-0.02	0.50	0.23	0.67	0.68	0.43	-0.50	-0.43	0.00	-0.03	-0.23	-0.46	-0.43	-0.40	-0.16	-0.36	0.58	0.33	0.47	0.62	0.56	0.59	0.51
PepDMd	-0.19	0.04	-0.12	0.04	-0.32	-0.32	-0.20	-0.21	0.11	0.10	-0.17	0.05	0.17	0.07	0.09	-0.31	-0.02	-0.02	-0.38	0.08	-0.38	-0.32	-0.38	-0.33	-0.11
PancDMd	-0.25	0.82	0.53	-0.53	-0.37	-0.37	-0.85	-0.92	0.88	0.91	-0.69	0.68	0.85	0.91	0.90	0.46	0.61	0.74	-0.05	0.35	-0.28	-0.72	-0.52	-0.79	-0.90
ViscDMd	0.26	-0.73	-0.57	0.29	-0.16	0.19	0.63	0.80	-0.71	-0.76	0.75	-0.67	-0.80	-0.75	-0.74	-0.26	-0.62	-0.66	0.39	-0.54	0.13	0.54	0.34	0.62	0.76
DMd	0.34	0.02	0.05	0.23	0.30	0.55	0.34	0.09	-0.19	-0.09	-0.25	0.24	0.09	-0.12	-0.09	-0.27	-0.08	-0.23	0.33	0.42	0.28	0.35	0.30	0.28	0.23
SolDH	-0.13	-0.19	-0.22	0.13	-0.27	0.10	0.10	0.11	-0.22	-0.23	-0.03	-0.18	-0.10	-0.24	-0.25	-0.02	-0.32	-0.26	-0.01	0.08	-0.11	0.07	-0.02	0.07	0.21
PepDH	0.01	0.04	-0.04	-0.19	0.10	-0.00	-0.08	-0.06	0.18	0.12	0.09	-0.01	0.00	0.12	0.14	-0.17	0.09	0.04	-0.10	-0.18	-0.06	-0.14	-0.08	-0.12	-0.16
PanDH	0.13	-0.78	-0.58	0.37	-0.06	0.38	0.76	0.84	-0.81	-0.78	0.71	-0.61	-0.79	-0.78	-0.77	-0.40	-0.71	-0.61	0.57	-0.50	0.30	0.75	0.51	0.79	0.84
kPan	-0.32	0.35	0.37	0.18	0.17	-0.47	-0.36	-0.39	0.44	0.44	-0.22	0.36	0.39	0.42	-0.42	-0.25	0.46	0.33	-0.33	0.27	-0.19	-0.41	-0.32	-0.42	-0.37
TotDH	0.19	-0.83	-0.67	0.39	-0.27	0.33	0.78	0.88	-0.85	-0.88	0.73	-0.74	-0.85	-0.88	-0.87	-0.42	-0.77	-0.65	0.48	-0.51	0.17	0.69	0.44	0.75	0.87

ate analysis of the CHO (ca. 1,485-950 cm^{-1}), Amide (1,710-1,485 cm^{-1}) and Lipid (1,810-710 cm^{-1} / 3,050-2,790 cm^{-1}) spectral regions of the four whole insect meals used in the study. The results revealed a clear separation of BSFL and BC; however, both MW and FC fell within the same 95%-confidence ellipse. These findings are surprising as univariate analysis showed a more similar spectral profile between both cricket species than with MW. Attending to the PC loadings (Supplementary Figure S1), we observed that PC1 is mainly driven by a positive correlation with the Amide and CHO regions, whereas PC2 is positively correlated to lipid-related and Amide regions, and negatively with CHO wavelengths. Therefore, differences found in CHO and Amide regions' global profile should explain the PCA plot outcome. A previous study also showed suitable discrimination between MW and BC when six different whole insect species were analysed (Mellado-Carretero *et al.*, 2019). In that case, differences between insects (which included crickets, beetle worms, and grasshopper) were driven mainly by lipid-related regions. In conclusion, the multivariate analysis of the whole FTIR profile reveals global differences between insect meals that could be overseen by quantitative analysis. This fact may contribute to the helpfulness of FTIR to rapidly classify insect-derived products, and avoiding fraud, as it has extensively demonstrated in the past for alternative food and feed products (Wielogorska *et al.*, 2018; Galvin-King *et al.*, 2020).

4 Conclusions

Whole-insect powders of black soldier fly, mealworm, field crickets, and banded crickets showed differences in the chemical composition that were reflected in the *in vitro* DM digestibility, and degree of protein hydrolysis. The application of FTIR and univariate quantitative analysis of spectral features demonstrated the potential to rapidly identify these differences between insect species, as seen by correlation analysis. Besides, the multivariate analysis of the FTIR profile by PCA revealed interactions between the insect species that helped discriminate between groups. Therefore, FTIR in combination with uni-and-multivariate-analysis can become a rapid technique to predict the chemical composition and quality of insect's powders intended for inclusion within animal feed formulations, while also preventing adulteration and fraud. Further analysis focusing on the effect of insect life stage, sex, strains, feed and/or rear-

ing conditions would maximise the possibilities of ATR-FTIR applicability.

Supplementary material

Supplementary material is available online at:
<https://doi.org/10.6084/m9.figshare.25886521>

Conflict of interest

The authors have no conflicts of interest to declare.

Funding

Financial support for this work has been provided by the Biotechnology and Biological Sciences Research Council (BBSRC) [grant number BB/T008776/1] as part of the Doctoral Training Partnership FoodBioSystems: biological processes across the Agri-Food system from pre-farm to post-fork.

References

- Antonialli-Junior, W., Tofolo, V. and Giannotti, E., 2007. Population dynamics of *Ectatomma planidens* (Hymenoptera: Formicidae) under laboratory conditions. *Sociobiology* 50: 1005-1013.
- Bai, M., Qin, G., Sun, Z. and Long, G., 2016. Relationship between molecular structure characteristics of feed proteins and protein *in vitro* digestibility and solubility. *Asian-Australasian Journal of Animal Sciences* 29: 1159-1165. <https://doi.org/10.5713%2Ffajas.15.0701>
- Balan, V., Hihai, CT., Cojocaru, FD., Uritu, CM., Dodi, G., Botezat, D. and Gardikiotis, I., 2019. Vibrational spectroscopy fingerprinting in medicine: from molecular to clinical practice. *Materials* 12: 2884. <https://doi.org/10.3390%2Fma12182884>
- Belanche, A., Weisbjerg, M., Allison, G., Newbold, C. and Moorby, J., 2013. Estimation of feed crude protein concentration and rumen degradability by Fourier-transform infrared spectroscopy. *Journal of Dairy Science* 96: 7867-7880. <https://doi.org/10.3168/jds.2013-7127>
- Benjakul, S. and Morrissey, M., 1997. Protein hydrolysates from Pacific whiting soil wastes. *Journal of Agricultural and Food Chemistry* 45: 3425-3430. <https://doi.org/10.1021/jf970294g>

Bernardi, R., Firmino, E., Pereira, M., Andrade, L., Cardoso, C., Súarez, Y., Antonialli-Junior, W. and Lima, S., 2014. Fourier transform infrared photoacoustic spectroscopy as a potential tool in assessing the role of diet in cuticular chemical composition of *Ectatomma brunneum*. *Genetics and Molecular Research* 13: 10035-10048. <https://doi.org/10.4238/2014.november.28.8>

Boisen, S. and Fernández, J., 1997. Prediction of the total tract digestibility of two energy in feedstuffs and pig diets by *in vitro* analyses. *Animal Feed Science and Technology* 68: 227-286. [https://doi.org/10.1016/S0377-8401\(97\)00058-8](https://doi.org/10.1016/S0377-8401(97)00058-8)

Bolous, S., Tännler, A. and Nyström, L., 2020. Nitrogen-to-protein conversion factors for edible insects on the Swiss market: *T. molitor*, *A. domesticus*, and *L. migratoria*. *Frontiers in Nutrition* 7. <https://doi.org/10.3389/fnut.2020.00089>

Bosch, G., Vervoort, K. and Hendriks, W., 2016. *In vitro* digestibility and fermentability of selected insects for dog foods. *Animal Feed Science and Technology* 221: 174-184. <https://doi.org/10.1016/j.anifeedsci.2016.08.018>

Boukil, A., Perreault, V., Chamberland, J., Mezdour, S., Pouliot, Y. and Doyen, A., High hydrostatic pressure-assisted enzymatic hydrolysis affect mealworm allergenic proteins. *Molecules* 25: 2685. <https://doi.org/10.3390%2Fmolecules25112685>

Campbell, M., Ortuño, J., Stratakos, A., Linton, M., Corcionivoschi, N., Elliott, T., Koidis, A. and Theodoridou, K., 2020. Impact of thermal and high-pressure treatments on the microbiological quality and *in vitro* digestibility of black soldier fly (*Hermetia illucens*) larvae. *Animals* 10: 682. <https://doi.org/10.3390%2Fani10040682>

Chia, S., Tanga, C., van Loon, J. and Dicke, M., 2019. Insects for sustainable animal feed: inclusive business models involving smallholder farmers. *Current Opinion in Environmental Sustainability* 41: 23-30. <https://doi.org/10.1016/j.cosust.2019.09.003>

Chieco, C., Morrone, L., Bertazza, C., Cappellozza, S., Saviane, A., Gai, F., Di Virgilio, N. and Rossi, F., 2019. The effect of strain and rearing medium on the chemical composition, fatty acid profile and carotenoid content in silkworm (*Bombyx mori*) pupae. *Animals* 9: 103. <https://doi.org/10.3390%2Fani9030103>

Commission Regulation (EU), 2021/1372 (2021). Official Journal of the European Union L 295: 1-17. https://www.legislation.gov.uk/eur/2017/893/pdfs/eur_20170893_adopted_en.pdf

Cruz-Angeles, J., María Martínez, L. and Vide, M., 2015. Application of ATR-FTIR spectroscopy to the study of thermally induced changes in secondary structure of protein molecules in a solid state. *Biopolymers* 103: 574-584. <https://doi.org/10.1002/bip.22664>

Dorion, K., Yu, P., McKinnon, J. and Christensen, D., 2009. Heat-induced protein structure and subfractions in relation to protein degradation kinetics and intestinal availability in dairy cattle. *Journal of Dairy Science* 92: 3319-3330. <https://doi.org/10.3168%2Fjds.2008-1946>

Galvin-King, P., Haughey, S. and Elliott, C., 2020. The detection of substitution adulteration of paprika with spend paprika by the application of molecular spectroscopy tools. *Foods* 9: 944. <https://doi.org/10.3390/foods9070944>

Gasco, L., Biancarosa, I. and Liland, N., 2020. From waste to feed: a review of recent knowledge on insects as producers of protein and fat for animal feeds. *Current Opinion in Green and Sustainable Chemistry* 23: 67-79. <https://doi.org/10.1016/j.cogsc.2020.03.003>

Janssen, R., Canelli, G., Sanders, M., Bakx, E., Lakemond, C., Dogliano, V. and Vincken, J.P., 2019. Iron-polyphenol complexes cause blackening upon grinding *Hermetia illucens* (black soldier fly) larvae. *Scientific Reports* 9: 2967. <https://doi.org/10.1038/s41598-019-38923-x>

Janssen, R., Vincken, J.-P., van den Broek, L., Fogliano, V. and Lakemond, C., 2017. Nitrogen-to-protein conversion factors for three edible insects: *Tenebrio molitor*, *Alphitobius diaperinus*, and *Hermetia illucens*. *Journal of Agricultural and Food Chemistry* 65: 2275-2278. <https://doi.org/10.1021/acs.jafc.7b00471>

Jayanegara, A., Yantina, N., Novandri, B., Laconi, E., Ramli, N. and Ridla, M., 2017. Evaluation of some insects as potential feed ingredients for ruminants: chemical composition, *in vitro* rumen fermentation and methane emissions. *Journal of the Indonesian Tropical Animal Agriculture* 42: 247. <http://dx.doi.org/10.14710/jitaa.42.4.247-254>

Johnson, J., 2020. Near-infrared spectroscopy (NIRS) for taxonomic entomology: a brief overview. *Journal of Applied Entomology* 144: 241-250. <https://doi.org/10.1111/jen.12732>

Khoshmanesh, A., Christensen, D., Perez-Guaita, D., Iturbe-Ormaetxe, I., O'Neill, C., McNaughton, D. and Wood, B., 2017. Screening of *Wolbachia* endosymbiont infection in *Aedes aegypti* mosquitoes using attenuated total reflection mid-infrared spectroscopy. *Analytical Chemistry* 89: 5285-5293.

Kovitvadhi, A., Chandang, P., Thongprajukaew, K., Tirawat-tanawanich, C., Srikacharm, S. and Chotimanothum, B., 2019. Potential of insect meals as protein sources for meat-type ducks based on *in vitro* digestibility. *Animals* 9: 155. <http://dx.doi.org/10.3390/ani9040155>

Krämer, A., Böttcher, C., Gudi, G., Stürz, M. and Schulz, H., 2021. Application of ATR-FTIR spectroscopy for profiling of non-structural carbohydrates in onion (*Allium cepa* L.) bulbs. *Food Chemistry* 260: 129978. <https://doi.org/10.1016/j.foodchem.2021.129978>

Leni, G., Soetemansm, L., Jacobs, J., Depraetere, S., Gianotten, N., Bastiaens, L., Caligiani, A. and Sforza, S., 2020. Protein hydrolysates from *Alphitobius diaperinus* and *Hermetia illucens* larvae treated with commercial proteases. *Journal of Insects as Food and Feed* 6: 393-404. <https://doi.org/10.3920/JIFF2019.0037>

Liu, B., Thacker, P., McKinnon, J. and Yu, P., 2013. In-depth study of the protein molecular structures of different types of dried distillers grains with solubles and their relationship to digestive characteristics. *Journal of the Science of Food and Agriculture* 93: 1438-1448. <https://doi.org/10.1002/jsfa.5912>

Liu, N., Zhao, L., Tang, L., Stobbs, J., Parkin, I., Kunst, L. and Karunakaran, C., 2019. Mid-infrared spectroscopy is a fast screening method for selecting *Arabidopsis* genotypes with altered leaf cuticular wax. *Plant, Cell & Environment* 43: 662-674. <https://doi.org/10.1111/pce.13691>

Liu, Z., Rady, A., Wijewardane, N., Shan, Q., Chen, H., Yand, S., Li, J. and Li, M., 2020. Fourier-transform infrared spectroscopy and machine learning to predict fatty acid content of nine commercial insects. *Journal of Food Measurement and Characterization* 15: 953-960. <https://doi.org/10.1007/s11694-020-00694-9>

Lopez-Santamarina, A., del Carmen Mondragon, A., Lamas, A., Manuel Miranda, J., Manuel Franco, C. and Cepeda, A., 2020. Animal-origin prebiotic based on chitin: an alternative for the future? A critical review. *Foods* 9: 782. <https://doi.org/10.3390%2Ffoods9060782>

Manditsera, F., Luning, P., Fogliano, V. and Lakemond, C., 2019. Effect of domestic cooking methods on protein digestibility and mineral bioaccessibility of wild harvested adult edible insects. *Food Research International* 131: 404-411. <https://doi.org/10.1016/j.foodres.2019.03.052>

Mantilla, S., Alagappan, S., Sultanbawa, Y., Smyth, H. and Cozzolino, D., 2020. A mid infrared (MIR) spectroscopy study of the composition of edible Australian green ants (*Oecophylla smaragdina*) – a qualitative study. *Food analytical methods* 13: 1627-1633. <https://doi.org/10.1007/s12161-020-01783-7>

Marono, S., Piccolo, G., Loponte, R., Di Meo, C., Attia, Y., Nizza, A. and Bovera, F., 2015. *In vitro* crude protein digestibility of *Tenebrio molitor* and *Hermetia illucens* insect meals and its correlation with chemical composition traits. *Italian Journal of Animal Science* 14: 3889. <https://doi.org/10.4081/ijas.2015.3889>

Mellado-Cerretero, J., García-Gutiérrez, N., Ferrando, M., Güell, C., García-Gonzalo, D. and De Lamo-Castellví, S., 2019. Rapid discrimination and classification of edible insect powders using ATR-FTIR spectroscopy combined with multivariate analysis. *Journal of Insects as Food and Feed* 6: 141-148. <https://doi.org/10.3920/JIFF2019.0032>

Meneguz, M., Schiavone, A., Gai, F., Dama, A., Lussiana, C., Renna, M. and Gasco, L., 2018. Effect of rearing substrate on growth performance, waste reduction efficiency and chemical composition of black soldier fly (*Hermetia illucens*) larvae. *Journal of the Science of Food and Agriculture* 98: 5776-5784. <https://doi.org/10.1002/jsfa.9127>

Milali, M., Sikulu-Lord, M., Kiware, S., Dowell, F., Corliss, G. and Povinelli, R., 2019. Age grading *An. gambiae* and *An. arabiensis* using near infrared spectra and artificial neural networks. *PLOS ONE* 14: e0209451. <https://doi.org/10.1371/journal.pone.0209451>

Poelaert, C., Beckers, Y., Despret, X., Portetelle, D., Francis, F. and Bindelle, F., 2016. *In vitro* evaluation of fermentation characteristics of two types of insects as potential novel protein feeds for pigs. *Journal of Animal Science* 94: 198-201. <https://doi.org/10.2527/jas.2015-9533>

Purschke, B., Meinlschmidt, P., Horn, C., Rieder, O. and Jäger, H., 2018. Improvement of techno-functional properties of edible insect protein from migratory locust by enzymatic hydrolysis. *European Food Research and Technology* 244: 999-1013. <https://doi.org/10.1007/s00217-017-3017-9>

Ribeiro, J., Lima, R., Maia, M., Almeida, A., Fonseca, A., Cabrita, A. and Cunha, L., 2019. Impact of defatting freeze-dried edible crickets (*Acheta domesticus* and *Gryllodes sigillatus*) on the nutritive value, overall liking and sensory profile of cereal bars. *LWT* 113: 108335. <https://doi.org/10.1016/j.lwt.2019.108335>

Ritvanen, T., Pastell, H., Welling, A. and Raatikainen, M., 2020. The nitrogen-to-protein conversion factor of two cricket species – *Acheta domesticus* and *Gryllus bimaculatus*. *Agricultural and Food Science* 29: 1-5. <https://doi.org/10.23986/afsci.89101>

Sánchez-Muros, MJ., Barroso, F. and Agugliaro-Manzano, F., 2014. Insect meal as renewable source of food for animal feeding: a review. *Journal of Cleaner Production* 65: 16-27. <https://doi.org/10.1016/j.jclepro.2013.11.068>

Sree, K., Bilawar, S., Thamburaj, S., Palanivel, R. and Kalakandan, S., 2022. Application of Fourier transform infrared spectroscopy for the comparison of genetically modified Maize from non-GM maize varieties. *The Pharma Innovation Journal* 11: 3731-3737.

Tani, C., Vaccari, L., Mitri, E. and Birarda, G., 2020. FTIR investigation on the secondary structure of type I collagen: New insight into the amide III band. *Spectrochimica Acta Part A: Molecular and Biomolecular Spectroscopy* 229: 118006. <https://doi.org/10.1016/j.saa.2019.118006>

Theodoridou, K. and Yu, P., 2013a. Effect of processing conditions on the nutritive value of canola meal and presscake. Comparison of the yellow and brown-seeded canola meal with the brown-seeded canola presscake. *Journal of the*

Science of Food and Agriculture 93: 1986-1995. <https://doi.org/10.1002/jsfa.6004>

Theodoridou, K. and Yu, P., 2013b. Application potential of ATR-FT/IR molecular spectroscopy in animal nutrition: Revelation of protein molecular structures of canola meal and presscake, as affected by heat-processing methods, in relationship with their protein digestive behaviour and utilization for dairy cattle. *Journal of Agricultural and Food Chemistry* 61: 5449-5458. <https://doi.org/10.1021/jf400301y>

Tiencheu, V., Womeni, H., Linder, M., Mbiapo, F., Villeneuve, P., Fanni, J. and Parmentier, M., 2012. Changes of lipids in insect (*Rhynchophorus phoenicis*) during cooking and storage. *European Journal of Lipid Science and Technology* 115: 186-195. <https://doi.org/10.1002/ejlt.201200284>

Van Soest, P., Robertson, J. and Lewis, B., 1991. Methods for dietary fiber, neutral detergent fiber, and nonstarch polysaccharides in relation to animal nutrition. *Journal of Dairy Science* 74: 3583-3597. [https://doi.org/10.3168/jds.S0022-0302\(91\)78551-2](https://doi.org/10.3168/jds.S0022-0302(91)78551-2)

Vandanjon, L., Burlot, AS., Zamanileha, E., Douzenel, P., Rabélonandro, P., Bourgougnon, N. and Bedoux, G., 2023. The use of FTIR spectroscopy as a tool for the seasonal variation analysis and for the quality control of polysaccharides from seaweeds. *Marine Drugs* 21: 482. <https://doi.org/10.3390/md21090482>

Wielogorska, E., Chevallier, O., Black, C., Galvin-King, P., Delêtre, M., Kelleher, C., Haughey, S. and Elliott, C., 2018. Development of a comprehensive analytical platform for the detection and quantitation of food fraud using a biomarker approach. The oregano adulteration case study. *Food Chemistry* 239: 32-39. <https://doi.org/10.1016/j.foodchem.2017.06.083>

Wilfart, A., Yaguelin-Peyraud, Y., Simmins, H., Noblet, J., Milgem, J. and Montagne, L., 2007. A step-wise *in vitro* method to estimate kinetics of hydrolysis of feeds. *Livestock Science* 109: 179-181. <https://doi.org/10.1016/j.livsci.2007.01.139>

Yu, P., 2005. Protein secondary structures (alpha-helix and beta-sheet) at a cellular level and protein fractions in relation to rumen degradation behaviours of protein: a new approach. *The British Journal of Nutrition* 94: 655-665. <https://doi.org/10.1079/bjn20051532>

Zhen, Y., Chundang, P., Zhangm, Y., Wang, M., Vongsangnak, W., Prusakorn, C. and Kovitvadhi, A., 2020. Impacts of killing process on the nutrient content, products stability and *in vitro* digestibility of black soldier fly (*Hermetia illucens*) larvae meals. *Applied Sciences* 10: 6099. <https://doi.org/10.3390/app10176099>

Zielińska, E., Baraniak, B., Karaś, M., Rybczyńska, K. and Jakubczyk, A., 2015. Selected species of edible insects as a source of nutrient composition. *Food Research International* 77: 460-466. <https://doi.org/10.1016/j.foodres.2015.09.008>